Changes in pools of organic matter and major elements in the soil following prescribed pastoral burning in the central Pyrenees

J.L. Mora[a], A. Girona–García[b], C. Martí–Dalmau[c], J.O. Ortiz–Perpiñá[c], C.M. Armas–Herrera[c] and D. Badía–Villas[c]

[a] Departamento de Ciencias Agrarias y del Medio Natural, Facultad de Veterinaria, Instituto de Investigación en Ciencias Ambientales (IUCA), Universidad de Zaragoza, C/. Miguel Servet 177, 50013 Zaragoza, Spain

[b] Centre for Environmental and Marine Studies (CESAM), Department of Environment and Planning, University of Aveiro, Aveiro 3810–193, Portugal.

[c] Departamento de Ciencias Agrarias y del Medio Natural, Escuela Politécnica Superior de Huesca, Instituto de Investigación en Ciencias Ambientales (IUCA), Universidad de Zaragoza, Ctra. Cuarte s/n, 22071 Huesca, Spain

ABSTRACT

High–mountain soils are rich in partially decomposed organic matter, which is highly sensitive to mineralization and fire. Prescribed burning is performed in the Pyrenees to keep subalpine grasslands open for grazing. The compositions of the ash, litter and duff layers, and the particulate organic matter (POM) of the topsoil in the 0–1, 1–2, 2–3, and 3–5 cm depths were analyzed in relation to the nutrient availability after the prescribed burning of a stand encroached by erizón (*Echinospartum horridum*). The concentrations of C, N, P, and S and organic components (nonstructural, hemicellulose, cellulose, and lignin–type) were determined before the prescribed burn and 0, 6, 12, 18, and 24 months after the prescribed burn. The fire consumed the aboveground biomass, the litter and part of the duff layer, and the most thermostable (i.e., lignin–type) components and the least volatile

elements (P, S) were selectively preserved in the resulting ash. Prescribed burning caused significant losses of organic–C (–72%) and of N (–68%) only in the 0–1 cm depth. The organic–C loss was mostly (82%) from the POM, whereas the N loss was from more similar proportions of the POM (57%) and the nonparticulate organic matter (NPOM) (43%). However, few changes were observed in the composition of the organic matter, which pointed to a largely uneven combustion that resulted in a substantial part of the organic matter remaining largely untouched by the fire. After 6 months, the duff layer was depleted in hemicellulose by 32% compared to immediately after the burn, and fragmentation of the POM into the NPOM was observed. During the second spring, N– and P–rich charred POM were incorporated into the top 1 cm, while C–rich charcoal particles underwent fragmentation and vertical transport into the deeper soil. The preburn ecosytem was limited by P, and likely also by S. The plant available N showed transient increases of 1.5–2.1 times the immediate postburn levels for nitrate–N at 12 months after burning, and of up to 10–20 times for ammonium–N at 18 months. In contrast, the concentrations of plant–available P and S gradually declined to 1.8–3.3 and 1.8–4.0 times, respectively, lower at 24 months after the burn. Results indicated that fire–induced increases in the nutrient availability can be short–lived in high–mountain habitats, but steadier and likely more persistent nutrient inputs can derive from the gradual breakdown of charred organic matter.

KEYWORDS litter, duff, particulate organic matter, mountain soils, ecological stoichiometry

1. INTRODUCTION

Fire is a major disturbance around the globe (Thonicke et al., 2001) and is one of the more accessible and powerful tools available for manipulating habitats through the removal of unwanted plant biomass (Kull, 2008). Fire has been used for millennia in the mountain areas of southern Europe to clear land for grazing, being largely responsible for the expansion of alpine and subalpine grasslands at the expense of woodlands (Favilli et al., 2010; González–Sampériz et al., 2017). In the Pyrenees, burning practices have remained until modern times as an indispensable tool for keeping the grazing lands open, and have resurged in recent years in the form of prescribed burns (Faerber, 2009). Fire considerably affects soils, either directly by heating the soil components during burning or indirectly due to the removal of plant cover and the subsequent erosion after the fire (Santin and Doerr 2016). Prescribed fires have been shown to have variable effects depending on the soil and vegetation conditions and on the fire type, but are generally considered less harmful to the soils than wildfires because of the limited intensity and severity and low soil heating (Alcañiz et al., 2018; Fernandes et al., 2013).

High–mountain soils are generally poor and are often shallow or skeletal, and their fertility depends to a large extent on the soil organic matter (SOM) and its role as a water reservoir, source of nutrients, support for root growth, and soil–structuring agent (Bojko and Kabala, 2017; Prietzel and Christophel, 2014). Due to the low temperatures in the environment, organic matter cycling in the high–mountain areas is slow, resulting in the accumulation and temporal immobilization of large reservoirs of carbon (C) (Bojko and Kabala, 2017; Ward et al., 2014) and nutrients (Gavazov, 2010; Weintraub, 2011), mainly in the form of particulate organic matter (POM), i.e., SOM larger than 50 μm (Puissant et al., 2017; Saenger et al., 2015). However, POM is generally labile, i.e., easily decomposable by

73 microorganisms, which makes these C and nutrient reservoirs sensitive to changes in the
74 climate or land management (García–Pausas et al., 2017; Hagedorn et al., 2010). Due to
75 their richness in POM, mountain soils can be particularly vulnerable to management
76 practices that have potential impacts on the C cycle and ecosystem performance (Bing et
77 al., 2016; Hagedorn et al., 2010).
78
79 Several recent studies have investigated the impact of prescribed pastoral fires on high–
80 mountain soils in the southern Pyrenees and have focused on microbiological and
81 biochemical properties (Armas–Herrera et al., 2018; Girona–García et al., 2018a, 2019;
82 Múgica et al., 2018), bioavailable nutrients (Girona–García et al., 2018c; Múgica et al.,
83 2018), and total C and nitrogen (N) reservoirs in the whole topsoil layer (Nuche et al., 2018;
84 Girona–García et al., 2019) and in different aggregate–size classes (Girona–García et al.,
85 2018b). However, little is known about the effects of high–mountain pastoral burns on the
86 composition and nutrient concentration of organic matter in the high–mountain soils.
87
88 Moreover, studies examining the effects of burning on nutrient reservoirs in POM are rare.
89 Soil POM mainly consists of hemicellulose, cellulose, and lignin–type structural
90 components, which are listed in increasing order of their stabilities against microbial
91 (Jensen et al., 2005; Kwiatkowska–Malina 2018) and thermal degradation (Yang et al.,
92 2007). When the fire intensity is not too large as is the case with prescribed fires, the
93 preferential preservation of the more resistant (i.e., lignin–type) fractions over the more
94 unstable fractions (hemicellulose, cellulose) can be expected (Fernández et al., 2001). Fire
95 will also likely cause more intense effects on free POM than on nonparticulate organic
96 matter (NPOM), which is chemically stabile and associated with soil minerals (Almendros
97 and González–Vila, 2012).

The aim of this study was to analyze the short–term (two–year) effects of prescribed burning on the composition and the nutrients contained in the organic matter near the soil surface and in the topsoil layer and on the nutrient availability in the topsoil in a subalpine pastureland area in the Pyrenees. It was hypothesized that (i) burning has greater effects on the most labile components of decomposing organic matter than on those more stable and on the POM than on the NPOM and that (ii) fire–induced mineralization of large amounts of organic matter would lead to increased nutrient availability immediately and shortly after burning.

2. MATERIAL AND METHODS

2.1. Experimental setting

Research was conducted in a subalpine summer pasture area located in Buisán–Fanlo (province of Huesca, Spain) in the south–central Pyrenees. The elevation at the study site is approximately 1760 m above sea level and the climate in the area is continental with some oromediterranean influence with a mean atmospheric temperature of 6 ˚C and mean rainfall of 1500 $mm \cdot year^{-1}$. The lithology is composed of calcareous Eocene rocks, including detrital sediments of limestone and marlstone. The slope is 10–25% and is exposed to the south. The soils are Calcaric Cambisols of varying thickness with a silt–loam texture in the top 5 cm and a clay–loam texture below 5 cm. During recent decades, the livestock density has decreased by approximately 50%, and undergrazing has resulted in a mosaic–patterned landscape, with nearly monospecific thickets of erizón [*Echinospartum horridum* (Vahl) Rothm.], a thorny shrub encroaching into grasslands dominated by mesophytic grasses such as common bent (*Agrostis capillaris* L.), quaking

grass (*Briza media* L.), erect brome (*Bromus erectus* Huds.), Chewing's fescue (*Festuca nigrescens* Lam.), and red clover (*Trifolium pratense* L.).

On 12 November 2015, the wildfire prevention team (EPRIF, the Spanish acronym) of Huesca and the firefighting reinforcement brigades (BRIF) of Daroca (Spain) conducted the prescribed burn of a nearly monospecific stand of *E. horridum* with an area of 3.8 ha (Fig. 1a). The shrub cover of the stand was 75%, and the fuel load was estimated at 9.2 kg m^{-2} from aboveground biomass and 1.6 kg m^{-2} from the litter (undecomposed or only slightly decomposed plant debris) and duff (partly decomposed organic matter) layers. The topsoil was moist at the surface (1.3–1.7 kg water·kg^{-1} dry soil in the 0–1 cm depth) and less moist below (0.5–0.8 kg water·kg^{-1} dry soil in the 1–5 cm depth). Burning was conducted under weak winds (< 8 km·h^{-1}) using a point–source technique; the shrubs were ignited one by one when the shrub cover was not continuous. Temperatures were recorded during burning at a single point on the soil surface and at depths of 1, 2, and 3 cm into the soil using k–type thermocouples. At the soil surface, a maximum temperature of 438 ˚C and a residence time with temperatures above 100 ˚C of 12.5 min were recorded, but the heating was only slight at the 1–cm depth (peak of 31 ˚C) and negligible at the 2– and 3–cm depths.

On the day of the burn, a smaller area was selected within the stand before burning, near, but not too close to, the starting ignition point, with sufficient soil depth to avoid rocks at or under the soil surface when sampling soils. Within the area, three microsites were selected that were separated by 5 m, as wide as possible and distant enough from rocks to avoid border effects, forming an upside–down equilateral triangle. The spacing was judged in the field to be enough to ensure sample independence, since the triangular design

147 prevented flows of runoff or sediments between the microsites. At each microsite, a 0.25–
148 m^2 surface was delimited, and samples were collected immediately before burning
149 (preburn) from the litter, duff, and topsoil. Litter was collected by hand–picking from the
150 ground surface. Then duff was obtained by gently scrapping the surface of the underlying
151 topsoil using a trowel. Finally, topsoil samples were obtained by digging with a trowel from
152 the 0–1, 1–2, 2–3, and 3–5 cm depths. Immediately after burning (T0), samples were
153 collected in adjacent 0.25–m^2 areas at the same microsites from the ash deposited on the
154 soil surface, the remaining duff layer, and the topsoil from the 0–1, 1–2, 2–3, and 3–5 cm
155 depths. Sampling of the duff and topsoil was repeated every six months over the two
156 following years in May 2016 (T6) (Fig. 1e), November 2016 (T12) (Fig. 1f), May 2017
157 (T18) (Fig. 1g), and November 2017 (T24) (Fig. 1h). The study used the preburn state as
158 the reference point of comparison to assess temporal changes, due to either the fire effects
159 or environmental conditions that vary with time, particularly from seasonal and weather
160 effects.
161
162 2.2. Laboratory procedures
163 Research aimed to assess changes in the composition of the organic matter and the labile
164 reservoirs of C, N, phosphorus (P), and sulfur (S) in the litter and duff layers and in the
165 POM within the topsoil layer. The nutrient status of the soil was also investigated through
166 analysis of the plant–available N, P, and S concentrations and related soil properties, such
167 as pH and electric conductivity. A schematic overview of the main analyses is provided in
168 Figure 2.
169
170 The litter, duff, and ash samples were dried at 60 ˚C in an oven to constant weight and were
171 ground using a cutting mill to pass a 1–mm sieve. Soil samples were divided into two parts:

one part was air–dried for 3–5 days until visibly dry, sieved to < 2 mm and stored at room temperature (18–25 ˚C), and the second part was sieved while still fresh and stored at 4 ˚C until analysis. For all samples, the water content was determined gravimetrically to constant weight in an oven at 103 ˚C. The total concentration of the organic matter was assessed from weight–loss–on–ignition at 550 ˚C for 4 h in a muffle furnace, and the total C and N concentrations were determined using a CN Vario Max elemental analyzer (Elementar, Hanau, Germany). For soil and ash samples, the calcium carbonate equivalent was determined by the volumetric method using a Bernard calcimeter (Proeti, Madrid, Spain), and the concentration of carbonate–C was subtracted from that of the total C to obtain the organic–C concentration.

The litter, duff, and ash were analyzed for the total concentrations of P and S by ashing in the presence of magnesium nitrate and redissolution in *2N* hydrochloric acid (Kalra and Maynard, 1991). The total P concentration was spectrometrically determined by the blue–molybdate method (Murphy and Riley, 1962) and the total S concentration was determined by turbidimetry with barium chloride (Rhoades, 1982). The organic composition of the litter, duff, and ash was assessed using an Ankom 200 Fiber Analyzer (Ankom Technol., Fairport, NY, USA) according to the Van Soest method, which uses neutral–detergent, acid–detergent, and 72% sulfuric acid solutions to sequentially determine the nonstructural (cell content), hemicellulose, cellulose, and lignin–type components of the organic matter, where lignin-type components include lignin as well as other substances with comparable recalcitrance, such as cutin, suberin or waxes (Berg and McClaugherty, 2014). The insoluble mineral residue was separated by ashing in a muffle furnace at 550 ˚C, and its concentration was subtracted from that of the lignin–type components.

The soils and ash were analyzed for chemical properties and nutrient concentrations. The pH was measured in a 1:2.5 air–dried soil:water or ash:water mass suspension, and the electric conductivity was measured in a 1:5 air–dried soil:water or ash:water mass extract. The bioavailable N in the forms of ammonium (ammonium–N) and nitrate (nitrate–N) was extracted from the fresh soil or from ash with a *2 M* potassium chloride solution at a 1:10 mass:volume ratio and was determined with steam distillation through the magnesium oxide–Devarda alloy method (Bremner, 1965). Plant–available P was extracted from the air–dried soil or ash following the Olsen procedure using a *0.5 M* sodium bicarbonate solution with pH 8.5 at a 1:20 mass:volume ratio (Watanabe and Olsen, 1965) and was spectrometrically determined by the molybdate–blue method (Murphy and Riley, 1962). The soluble (plant–available) S was determined in the 1:5 mass:volume aqueous extract by turbidimetry with barium chloride (Rhoades, 1982).

For the POM analysis, soil subsamples were dispersed using a sodium hexametaphosphate solution, and the sand–sized fraction was separated using a 50–μm sieve. From the sand–sized fraction, a portion was ground using a mortar and was analyzed for POM, C [particulate organic–C (POC)] and N [particulate organic N (PON)] concentrations following the methods described above. Another part was placed in water and stirred to separate the floating POM from the mineral sand (Saenger et al., 2015). In the isolated POM, the total P [particulate organic P (POP)] and S [particulate organic S (POS)] concentrations and the nonstructural, hemicellulose, cellulose, and lignin–type organic fractions were determined using the methods described above.

2.3. Data processing and statistical analyses

Results of the analyses were expressed in concentration units on a mass per oven–dry mass basis. The concentrations of nonstructural, hemicellulose, cellulose, and lignin–type components were expressed as percentages of the total (ash–free) organic matter. The concentrations of the POC, PON, POP, and POS were expressed on a mass per mass of total soil basis. The values of nonparticulate organic–C (NPOC) and nonparticulate organic N (NPON) were obtained by subtracting the POC and PON concentrations from the total concentrations of soil organic–C and N. The C:N, C:P, C:S, N:P, N:S, and P:S stoichiometric mass ratios were calculated for the litter, duff, ash, and POM and the C:N ratio was calculated for the NPOM.

The initial weight loss resulting from the combustion and volatilization of the soil components during burning was calculated for each of the soil depths from the total SOM values, according to the following formula [Eq. (1)]:

$$Mass\ loss = 1000 \times \frac{SOM_{preburn} - SOM_{T0}}{1000 - SOM_{T0}} \quad (1)$$

where the weight loss is expressed as g·kg^{-1} initial concentration, and $SOM_{preburn}$ and SOM_{T0} are the SOM concentrations just before and after burning, expressed as g·kg^{-1} soil. The weight loss resulted in the apparent enrichment of any remaining components in the soil after burning, which was estimated with the following calculation [Eq. (2)]:

$$Concentration\ effect = \frac{1000}{1000 - Mass\ loss} \quad (2)$$

Taking into account the concentration effect, the actual losses of total N, P, and S from the POM were estimated using the following calculation [Eq. (3)]:

$$\Delta(N,P,S) = \frac{POM_{preburn} \times PO(N,P,S)_{preburn}}{1000} - \frac{POM_{T0} \times PO(N,P,S)_{T0}}{1000 \times Concentration\ effect} \quad (3)$$

and of total N from the NPOM according to the following calculation [Eq. (4)]:

$$\Delta N = \frac{NPOM_{preburn} \times NPON_{preburn}}{1000} - \frac{NPOM_{T0} \times NPON_{T0}}{1000 \times Concetration\ effect} \quad (4)$$

where $POM_{pre-burn}$, POM_{T0}, $NPOM_{pre-burn}$, and $NPOM_{T0}$ are the concentrations of POM and NPOM before and after burning, expressed as $g \cdot kg^{-1}$ soil; *PO(N, P, S)* and *NPON* are the total concentrations of N, P, and S in the POM and of N in the NPOM, expressed as $mg \cdot kg^{-1}$ organic matter; and $\Delta(N, P, S)$ and ΔN are the losses estimated in $g \cdot kg^{-1}$ initial soil.

The changes in the composition of the duff and the topsoil over the study period (preburn, T0, T6, T12, T18, and T24) across the distinct layers (duff and topsoil at 0–1, 1–2, 2–3, and 3–5 cm depths) were analyzed using a linear mixed model of repeated measures in IBM SPSS Statistics v. 22 (IBM Corporation, Armonk NY, USA).

An initial model was built including time and layer as fixed effects, and the sampling microsite within the stand as a random effect to deal with the risk of spatial dependence. For each variable, the corrected Akaike information criterion (AICc) and the Bayesian information criterion (BIC) were used to select the best model among various alternatives. Thus, the AIC and BIC were used to test for the need of the random "microsite", for which models either including or not the random "microsite" term were compared (Supplementary Table 1). Lower AIC and BIC values were obtained when the random factor was included than when not included (with the only exceptions of the models for some stoichiometric ratios), which indicates that the soil properties varied across the microsites, hence the inclusion of the random term was fully justified. The AICc and BIC were also used to determine the most suitable covariance structure (Onyiah, 2008), which was a first–order self–regressive structure in all cases. The assumptions of normality and homoscedasticity were checked through Shapiro–Wilk tests and visually with residual plots, and, when necessary, the variables were square root– or log–transformed for statistical analyses.

In almost all cases, the interaction between the factors time and layer was statistically significant or near significant at $P < 0.05$ (Supplementary Table 2). Given interactions, examining the simple effects of one of the factors in the interaction at the individual levels of the other factor is recommended (Onyiah, 2008). Because the focus of this study was on temporal changes, all analyses were repeated separately for each layer through consideration of only the microsite and time factors. The results of the analyses for the effects of time on the individual layers are shown in Supplementary Table 3. When significant differences were identified for time, pairwise comparisons were performed with Bonferroni tests at $P < 0.05$. For ease of interpretation, means given in the results were based on the nontransformed data.

3. RESULTS

3.1. Characteristics of the ground surface and vegetation

Fire almost completely consumed the aboveground biomass and the litter layer (Fig. 1a, b). After burning, the soil surface was covered with a mix of unconsumed material from the duff layer (Fig. 1c) and ashes of various colors (white, gray, black) indicative of an irregular fire intensity (Fig. 1d), which were intercalated with some patches of bare ground.

The ash produced by the fire was alkaline in nature and was rich in carbonates and soluble substances (Table 1). The concentration of the organic matter was less than 20% and was proportionally rich in recalcitrant (lignin–type) components and much poorer in the most labile (hemicellulose, nonstructural) components. On average, 22% of the total S, 4% of total P, and 0.7% of total N in the ash were in forms available to plants.

Six months after the burn (Fig. 1d), i.e. after the winter and snow–covered periods, a large amount of burnt residue remained at the soil surface, covering 90% of the area. At 12

295 months after burning (Fig. 1e), mixed ash and duff material and limited incorporation of
296 charred organic matter into the topsoil were noticeable. Plant recolonization (as shown in
297 Fig. 1e, 1f, 1g, 1h) started slowly (5% cover after 6 months), but spread to most of the land
298 surface after 24 months (Fig. 1h). The recolonizing vegetation was dominated by plants
299 that resprout from rhizomes or bulbs, such as glaucous sedge (*Carex flaca* Schreb.), dwarf
300 sedge (*C. humilis* Leysser), cypress spurge (*Euphorbia cyparissias* L.), English iris [*Iris*
301 *latifolia* (Mill.) Voss.], wall germander (*Teucrium chamaedrys* L.), and Teesdale violet
302 (*Viola rupestris* F.W. Schmidt), along with *E. horridum*, which sprouts from seeds.
303
304 3.2. Organic compositions of the litter, duff, and topsoil
305 The litter and duff layers had similar organic compositions before the burn and differed
306 mainly in that the lignin–type components were at a greater concentration in the duff than
307 in the litter matter (Fig. 3). Burning removed the litter layer, but most of the duff layer
308 remained at the soil surface (Fig. 1c, 1d). During the study period, the composition of the
309 duff layer showed little change, except for a tendency toward selective preservation of the
310 most–recalcitrant polymers over time (Fig. 3). Indeed, the hemicellulose concentration
311 decreased slightly, but significantly at T6 and T24 compared to preburn and T0, whereas
312 the cellulose concentration increased by T24 compared to preburn. The lignin–type
313 predominant fraction did not change.
314
315 Burning did not immediately affect the organic composition of the topsoil. During the study
316 period, early (T6) and late (T24) enrichments in the lignin–type components were recorded
317 in the 0–1 cm depth. Similarly, the proportions of nonstructural components in organic
318 matter significantly increased first (T12) in the 3–5 cm and afterwards (T18) in the 1–2 and

2–3 cm depths. The NPOM changed little during the study period, showing only a decrease in its relative proportion in the 3–5 cm depth at T12.

3.3. Elemental composition of the organic matter

The topsoil underwent an average loss of 71% of its total SOM (POM + NPOM) in the 0–1 cm depth (Fig. 4a). The loss equaled 39% of the soil mass in the top 1 cm before burning and resulted in an apparent enrichment of 65% of the soil components remaining after burning, solely as a result of their concentration in the burned soil. The total organic–C and N underwent mean losses of 72% (Fig. 4b) and 68% (Fig. 4c), respectively, of their preburn concentrations in the same depth. Burning most severely impacted the POM, which accounted for 73% of the total loss of organic matter, 82% of the total C loss, and 60% of the total N loss, on average. Conversely, the NPOM only lost 27% of its initial concentration, which, added to the mass–concentration effect, caused its concentration in the soil to increase from 321 ± 31 $g \cdot kg^{-1}$ to 463 ± 109 $g \cdot kg^{-1}$ (mean ± standard deviation) after burning. In the underlying soil, the 1–2, 2–3, and 3–5 cm depths, the changes in SOM as result of burning were much lower, resulting in little or no concentration effect (+4%, +0%, and –0%, on averages).

The combustion of the POM and NPOM in the 0–1 cm depth released, on average, 12 g of N per kg of initial soil, of which 57% was released from the POM and 43% from the NPOM. From the POM alone, 0.17 g P kg^{-1} and 0.44 g of $S \cdot kg^{-1}$ initial soil were released, on average. The N, P, and S releases were approximately 120, 40, and 7.5 times larger, respectively, than their bioavailable concentrations before burning in the 0–1 cm depth. Despite this, no noticeable increases were observed in the concentrations of bioavailable N or P immediately after burning. An increase in the soluble concentration of S was observed,

344 although the increase was 12 times smaller than the amount of S released from the POM
345 combustion.
346
347 The immediate impact of burning on the POC concentration was followed by further losses
348 during the first months after burning and the POC concentration reached the lowest in the
349 0–1 and 1–2 cm depths at T6 (Fig. 5a). The NPOC concentrations decreased significantly
350 in the 0–1 and 1–2 cm depths just after burning, but increased at T6 up to levels that were
351 no longer lower than the preburn levels. The NPOC reached its greatest concentration at
352 T18 after burning, which was statistically significant in the 2–3 and 3–5 cm depths. Like
353 the POC, the PON decreased during the first months following burning in the 0–1 and 1–2
354 cm depths, reaching its significantly lowest concentrations at T6 and greatest
355 concentrations at T18 (Fig. 5b). In contrast, the NPON in the 0–1 cm depth, unlike the
356 NPOC, did not show a fast recovery, but continued to decrease after burning, reaching a
357 minimum at T12, and did not revert to preburn levels during the study period. No changes
358 over time occurred for PON or NPON at greater depths. The soil POP concentrations (Fig.
359 5c) did not decrease as a result of burning and showed transient variations during the study
360 period, reaching its lowest concentrations at T6 and its maximum concentrations at T18.
361 The POS concentration (Fig. 5d) decreased at T0 to its lowest concentration in the 0–1 cm
362 depth, which were significantly lower than the preburn, T18, and T24 concentrations.
363 Conversely, POS concentration in the 1–2, 2–3, and 3–5 cm depths was lowest at preburn,
364 then increased thereafter until reaching larger concentrations at T18.
365
366 The C:N ratio of the duff layer (Fig. 6a) did not show significant variations during the study
367 period. The C:N ratio of the POM decreased significantly in all depths at T6 and at later
368 sampling times, whereas the C:N ratio of the NPOM increased. The C:P ratio (Fig. 6b) was
369 lowest for the duff layer at T0 and increased significantly to the largest values at T18,

whereas the C:P ratio of the POM was largest before burning and decreased significantly at T6 in the 0–1 cm depth and at T18 in the 1–2, 2–3, and 3–5 cm depths. The C:S ratio (Fig. 6c) increased in the duff at T6 and decreased in the POM at T6. The N:P ratio (Fig. 6d) was largest in the duff layer at T18, when it was significantly greater than that preburn. In contrast, the N:P of the POM was lowest at T18, when its values were significantly lower than that preburn in the 0–1 cm depth and generally lower than those at T12 and T24. The N:S ratio (Fig. 6e) of the duff layer tended to increase after T6; the values at T18 were significantly lower than the preburn values. The N:S ratio of the POM did not show significant variations during the study period. Finally, the P:S ratio (Fig. 6f) increased after the burn until reaching values significantly greater than the initial values in the duff at T12 and in the POM at T18.

3.4. Soluble and plant–available elements

Electrical conductivity was observed to increase significantly in the top 3 cm of the soil (Fig. 7a) immediately after burning (T0). The largest conductivity was observed at T0 and T12 and was larger than that at T6 in the 0–1 cm depth and that at T24 in the 1–2 and 2–3 cm depths. The soil pH (Fig. 7b) remained alkaline (7.4–7.7) during the entire study period and was only affected by burning at T0 in the 0–1 cm depth when pH was slightly, but significantly greater than preburn, T6, T18, and T24 values. The calcium carbonate equivalent did not differ during the study period and was significantly lower in the 0–1 cm depth (82 ± 65 g·kg^{-1} than in greater (1–5 cm) depths (115 ± 73 g·kg^{-1}).

The concentrations of ammonium– and nitrate–N showed large variability before burning, which made their changes immediately after burning undetectable. Ammonium–N (Fig. 7c) increased postburning until peaking at T18 before decreasing at T24. Apart from this trend,

the spring ammonium–N concentrations were generally, though not significantly, greater than those of the preceding autumn. For nitrate–N (Fig. 7d), the largest values in the 2–3 and 3–5 cm depths were reached at T6, and the largest concentrations in the 0–1 and 1–2 cm depths were reached at T12. There was a sharp decrease at T18, although the concentrations seemed to increase again, though not significantly, at T24. In this case, the autumn concentrations were generally, though not significantly, greater than those in the preceding spring. The plant–available P (Fig. 7e) did not vary during burning, but decreased gradually thereafter in all depths, reaching its minimum concentrations at the end of the study period (T24). Within the general decline, the concentrations were numerically, though not significantly, greater in spring (T6, T18) than in autumn (T12, T24). At T0, the soluble S (Fig. 7f) reached its maximum concentration, which was significantly greater than the preburn concentrations in the 0–1 cm depth. Soluble S concentrations decreased with time since burning in the 1–2, 2–3 and 3–5 cm depths, reaching their minimums at T24. In addition, concentrations were generally, though not significantly, greater in autumn (T12, T24) than in spring (T6, T18).

4. DISCUSSION

4.1. Direct effects of fire on the organic layers

The maximum temperature recorded at the soil surface (438 °C) was intermediate between the characteristic temperatures for the formation of black carbon (approximately 350 °C) and for complete ashing (550 °C) (González–Pérez et al., 2004) and were sufficient to produce the formation of calcite from organic–C and Ca and the partial volatilization of N and S, but not of P (Bodí et al., 2014). The combustion produced an ash material where the organic matter was a minor component that was dominated (69%) by lignin–type components. The ash composition contrasted with that of the litter before burning, where

the lignin–type components accounted for 30% of the organic matter and that reported for the fine twigs of *E. horridum* (Marinas et al., 2003; Mora et al., 2018), where these components ranged from 15 to 18% on average. The larger concentration of lignin–type components in the ash indicated a selective preservation of the lignin–type components, likely as result of their lower flammability, greater resistance to heat and ease of carbonization in comparison with the other structural polymers in plants (Yang et al., 2007). These results were consistent with the decreasing concentration of O–alkyl C, which has been reported in ^{13}C nuclear magnetic resonance analyses of the burning of litter and is attributed to the intense thermal degradation of hemicellulose and cellulose (Alexis et al., 2010; Merino et al., 2015). However, compared with litter, the ash had only slightly lower concentrations of cellulose but much lower concentrations of hemicellulose, which likely reflected a lower contribution to the ash from the litter and duff layers than from the biomass of *E. horridum*, where the cellulose concentration was double that of the hemicellulose (Marinas et al., 2003; Mora et al., 2018).

With respect to the elemental composition, the ash had N, S, and P total concentrations that were 2.1, 6.7, and 36 times lower, respectively, than that in the litter before burning and 2.3, 20, and 26 times lower than the fine twigs of *E. horridum* (Marinas et al., 2003; Mora et al., 2018). These results highlighted a lower loss of total P relative to S, of S relative to N, and of N relative to C, which was consistent with their different volatilization temperatures. As a consequence, the ash was depleted in mineral N, but rich in soluble, plant–available S, even though some of the S that may have been insolubilized by contact with the carbonates under the alkaline conditions of the ash (Pereira et al., 2019). Due to its high volatilization temperature, P was abundant in ash, but only a small part was in a form available for plants. The ratio of the bioavailable P to the total P has been reported to

445 decrease in ash with increasing temperatures as inorganic phosphate ions become bound to
446 cations in the ash, forming insoluble metal phosphates (Caon et al., 2014; Gray and
447 Dighton, 2006).
448
449 However, the burning of the duff layer did not modify the proportions of the distinct
450 fractions in the organic matter or the elemental stoichiometry. These results could be related
451 to the uneven incidence of fire in the duff layer, which may, in some cases, have been
452 completely removed, while in others, was preserved, possibly with few changes to its
453 composition. Results from this study were in agreement with those of other studies (e.g.,
454 Alexis et al., 2010; Butler et al., 2017), which reported few differences between the
455 composition of the litter before burning and that remaining at the soil surface and
456 emphasized the influence of unburnt organic matter on the composition of the organic
457 layers after the application of prescribed burning.
458
459 4.2. Direct effects of fire on the topsoil
460 Burning considerably affected the upper 1 cm of the topsoil, whereas, at greater depth, the
461 immediate effects on the soil properties were minimal or insignificant. This result was in
462 agreement with several studies on the effects of burning shrublands (e.g., Neary et al., 1999;
463 Caon et al., 2014) or controlled burning under laboratory conditions (Badía –Villas et al.,
464 2014), which reported no element volatilization from below 2 cm.
465
466 Results showed that C losses came mostly (82%) from the combustion of POM, but the
467 release of N came from both the POM and NPOM in comparable proportions (57% and
468 43%, respectively) because of the greater concentration of total N in NPOM in comparison
469 to that in the POM (Fig. 6a). Most of the released N was lost through volatilization from

the soil, as judged by the lack of significant increases in the levels of the mineral N in the soil after burning.

The release of S was estimated from only the POM, but a considerable release of S may have also occurred from the NPOM, since, as with N, S is usually more abundant in NPOM than in POM, especially in soils from cool climates (Amelung et al., 1998). The S release was associated with an increase in S concentration in soluble, plant–available forms, but the increase was approximately 40 times lower than the estimation of the S released from the POM in the 0–1 cm depth in this study. Significant S immobilization was unlikely to have occurred since the immobilization of this element normally takes places at pH values close to 12 (Pereira et al., 2019), which was much greater than the pH of the topsoil in the 0–1 depth, which ranged from 7.3–7.8. Thus, it can be deduced that most of the mineralized S was lost through volatilization from the soil. The loss of S from the upper soil layer is generally not expected in low– or moderate–intensity fires (Neary et al., 1999) because soil temperatures rarely rise enough in those fires to generate S losses from the topsoil (Tiedemann, 1987).

The P released from the POM, to which an unknown amount of P released from NPOM should be added, did not immediately increase the concentration of the plant–bioavailable P in the soil. This may be due to increase in the pH in the 0–1 cm depth, which at the calcareous study site might contribute to making P unavailable via calcium fixation. The P enrichment may have also been partially overridden by the loss of some amount of P in the form of fine–ash particles, which are highly susceptible to removal from a site by convection in the smoke columns during fire (Raison et al., 1985). Ash is highly enriched in low–volatile elements, hence ash transport in the smoke can result in substantial P export

(Raison et al., 1985). Dense smoke was observed during burning (Fig. 2b) and is typical when densely branched, shrub thickets are burned (Bell and Adams, 2008).

Few variations were identified in the proportions of the distinct fractions of the SOM in the 0–1 cm depth as a result of burning, which contrasted with the results of other studies that reported a preferential removal of carbohydrates and selective preservation of lignin and humified SOM (Badía–Villas et al., 2014; Jiménez–Morillo et al., 2016). In this study, it was likely that, as in the duff layer, the most surficial layer of the topsoil experienced uneven exposure to the fire, leading to an almost complete removal of the SOM in some areas, but resulted in few significant effects in the SOM in other areas. Furthermore, some of the organic matter may have been protected within the soil aggregates, which was consistent with the results presented for this same burn by Girona–García et al. (2018b) who reported fewer fire effects on the SOM in those soil fractions with greater degrees of aggregation.

4.3. Postburn evolution of the organic composition

During the first two years following the burn, the composition of the duff layer remained fairly stable. The main observable trend was the decrease in the hemicellulose by the spring after the first winter after burning (T6). Hemicellulose is most labile among the major components of litter and has been reported to be actively degraded during the first year after exposure to fire (Pyke, 2003). At the same time (T6), the C in the topsoil was affected by a disintegration process, as can be inferred from the decrease in POC and increase in NPOC. A similar process likely affected the POP, which also reached its minimum concentration by T6. Because the microbial biomass of the topsoil was severely affected by the burn (Girona–García et al., 2018a), such disintegration can be related to physical mechanisms,

such as gelifluxion and cryoturbation, which play important roles in the breakdown of charcoal in soils in cold regions (Preston and Schmidt, 2006). Physical alteration, however, did not affect the N within the POM or the NPOM, as was also observed by Naisse et al. (2015), who attributed the result to the greatest N stability within the heterocyclic aromatic structures in the charcoal.

In the second spring (T18), a large incorporation of sand–sized, N–rich ash into the shallowest part of the topsoil occurred, which manifested as increases in the POC and PON in the 0–1 and 1–2 cm depths. Simultaneously, in 1–2 and 2–3 cm depths, enrichment in fine C–rich organic particles occurred, as evidenced by the increases in the NPOC, but not in NPON, and large C:N ratios. The fine particles may have resulted from the breakdown of the particulate charcoal and the subsequent transport to deeper soil layers by drainage and/or cryoturbation (Hobley, 2019).

In contrast, the hemicellulose and the nonstructural components of the POM increased in the 3–5 cm depth at T12 and extended to shallower depths (1–2 and 2–3 cm depths) at T18. The low thermal stability of these compounds makes it unlikely that they were of pyrogenic origin, and their spreading from the subsoil suggests that they probably originated from the belowground biomass of the plants that resprouted via rhizomes and bulbs, which were observed to be predominant in the recolonizing vegetation. Hemicelluloses and nonstructural carbohydrates act as mobile reservoirs of energy and nutrients for many plants and play an important role in the capacity for resprouting after burning (Martínez–Vilalta et al., 2016).

4.4. Stoichiometric effects

Mora et al. (2018) analyzed the major nutrients in the fine twigs of *E. horridum* in the study region, obtaining an average N:P ratio of 46, which was well above the threshold of 16–20 for P limitation (Güsewell, 2004; Koerselman and Meuleman, 2006). In this study, the litter layer, which mainly consisted of fine twigs, showed a similar N:P ratio of approximately 53, which related to the symbiotic N inputs of leguminous plants and to the presence of calcite in the soil, which favors the retrogradation of P into forms that are not plant–available. Mora et al. (2018) also reported an average N:S ratio of 6.5, which was much lower than the recommended critical ratio of 17 (Kozłowska–Strawska and Kaczor, 2009), indicating a greater limitation of S relative to N. In the present study, greater N:S ratios (16.5 on average) were measured in the litter, suggesting strong resorption of S during senescence, which was consistent with a strong plant S demand. Total S concentrations were also observed to decrease in the organic matter from the litter to the duff layer, which pointed to a large microbial S demand. Both findings were indicative of a certain degree of S limitation in the preburn ecosystem.

The stoichiometric ratios of the decomposing organic matter provide insight into the ease with which the contained nutrients can be mobilized (Prescott, 2005; Berg and McClaugherty, 2014). In this study, the C:N ratio averaged approximately 30 in the litter, approximately 20 in the duff during the entire study period and approximately 20 in the POM immediately before and after burning. According to the criteria compiled by Prescott (2005), these values allow for a moderate release of N. Furthermore, since T6, the C:N of the POM decreased to mean values ranging from 5 to 13, allowing even faster N mobilization, which coincided with the largest levels of nitrate–N that were observed at T6 and T12.

In the case of the C:P ratio, the litter showed large initial values, with an average close to 1600. The duff also showed large values before burning (700 on average), immediately after the fire (400) and, especially after the fire (700 to 1400). The POM had C:P ratios between 400 and 1200 before burning. All of these values indicate a low capacity for P release. After burning, the C:P of the POM sharply decreased to between 40 and 200 between T6 and T18, indicating large potential for P mobilization. This phenomenon showed signs of weakening at T24, when large C:P ratios, 300 to 400 in the 0–1 and 1–2 cm depths, were measured again.

The N:P ratio of the POM was observed to decrease to below 15 at T18, which indicated a switch in the nutrient limitation from P to N at this time (Prescott, 2005). It is well known that the incorporation of P–rich, charred materials into the soil can induce a shift from P to N limitation after fire (Toberman et al., 2014), which has led to recognize fire as an essential element for maintaining productivity in P–limited ecosystems (Dijkstra and Adams, 2015; Butler et al., 2017). In this study, the shift in limitation was short–lasting, as the N:P ratio increased in the next sampling period (T24), although the increase occurred in autumn, when large quantities of nutrients were immobilized by microorganisms. Microorganisms are known to immobilize large quantities of key elements, such as P (Weintraub, 2011), which has been suggested to affect low–nutrient habitats beyond the simple effect of the ash layer (Huang et al., 2013). This result was in agreement with the observations by Múgica et al. (2018) in the western Pyrenees, who reported temporary increases in plant–bioavailable N only during the first year after fire, but identified more persistent (> 18 months) effects in increasing the N concentration in the microbial biomass and decreasing the microbial N demand.

595 4.5. Postburn evolution of soil nutrient availability

596 Results of this study showed tightly inter–related seasonal variations of low statistical
597 significance in the plant–available concentrations of N, P, and S in the topsoil, which
598 pointed to a greater concentration of ammonium–N and available P in spring and nitrate–
599 N and soluble S in autumn. The variations mirrored the typical seasonal oscillations of plant
600 and microbial nutrient resources in high–mountain habitats. For example, during spring
601 snowmelt, high–mountain soils receive considerable nutrient inputs from the release of the
602 nutrients immobilized in the microbial biomass since autumn and from the discharge of
603 nutrients mineralized by microorganisms during winter (Bardgett et al., 2005). However,
604 melting is associated with intense leaching, so more soluble nutrients, such as nitrate–N
605 (Hagedorn et al., 2001; Clement et al., 2012) or soluble S, are removed, whereas other less
606 mobile nutrients, such as ammonium–N (Makarov et al., 2010; Clement et al., 2012) and P
607 (Costa et al., 2019), are retained. During summer, nutrients are taken up in large amounts
608 by plants (Bardgett et al., 2005), but the nitrate concentrations increase in summer and until
609 autumn due to nitrification (Makarov et al., 2010), while sulfate concentrations can increase
610 due to the deposition of S–rich aerosols in the Pyrenean ranges during summer (Ripoll et
611 al., 2015).

612

613 Seasonal soil nutrient dynamics superpose and interact with the fire effects. Thus, during
614 the second spring (T18), the maximum ammonium–N concentration coincided with the
615 incorporation of large amounts of N–rich ash into the soil. Likewise, the minimum l nitrate–
616 N concentrations occurred at the same time as the translocation of the fine particles of
617 pyrogenic organic matter, which were both caused by intense leaching that accompanied
618 snowmelt. In general, the increases in the N availability that could be attributed to burning
619 were short–lived and rapidly reverted back to preburn levels during the following few

620 months. For the soluble S and plant–available P concentrations, in contrast, the apparent
621 trend was a gradual decline after burning, where both reached their minimum
622 concentrations by the end of the study period (T24).
623
624 5. CONCLUSIONS
625 The analysis of the ash that resulted from the burning revealed a strong enrichment in the
626 most recalcitrant (lignin–type) fractions and the least–volatile elements (S and especially
627 P) relative to those of the plant biomass and the litter and duff layers. There was also a
628 much greater effect of burning on the POM than on the NPOM in the topsoil. These results
629 supported the hypothesis that the different thermal stabilities of the organic components
630 should lead to a heterogeneous effect of the controlled burn on the organic matter. The
631 effects of combustion on the NPOM, despite being minor, were responsible for releasing
632 large amounts of elements, such as N and S, that are more abundant in NPOM than in POM.
633 In contrast, the organic matter that remained at the soil surface and in the topsoil after
634 burning showed only slight changes relative to that before burning, which could be related
635 to an uneven influence of burning, as a result of which some of the organic matter was
636 maintained with few or no modifications.
637
638 The investigated habitat was shown to be P–limited, following the study area's calcareous
639 nature, and also likely S–limited. The immediate effects of burning included strong N and,
640 to a lesser degree S, volatilization from the organic matter and the immobilization of P into
641 forms unavailable to plants. During the two years following burning, the bioavailable
642 concentrations of the studied nutrients showed short–lived increases in N or gradual
643 decreases in S and P, which were likely related to the strong demand for these elements
644 from microorganisms and plants and, probably, to intense leaching. More consistently, the

soil nutrient status was also modified by the incorporation and breakdown of nutrient–rich ash particles during the first year and especially during the second year after burning. The gradual disintegration of the particulate charcoal and its transport to depth by cryoturbation and/or leaching may have extended the effect of burning on the nutrients to beyond the period for which the effects on bioavailable concentrations were observed.

ACKNOWLEDGEMENTS

We thank Rosa Herrero Bernal for her support and collaboration in the laboratory work. This research was funded by the projects CGL2016–76620–R of the Spanish Ministry of Economy and Competiveness and JIUZ–2015–TEC–11 of the Ibercaja Foundation in collaboration with the University of Zaragoza. Thanks are also due for the financial support to CESAM (UID/AMB/50017–POCI–01–0145–FEDER–007638), to FCT/MCTES through national funds (PIDDAC), and the co–funding by the FEDER, within the PT2020 Partnership Agreement and Compete 2020.

REFERENCES

Alcañiz, M., Outeiro, L., Francos, M., Úbeda, X., 2018. Effects of prescribed fires on soil properties: A review. Sci. Total Environ. 613, 944–957. https://doi.org/10.1016/j.scitotenv.2017.09.144

Alexis, M.A., Rumpel, C., Knicker, H., Leifeld, J., Rasse, D., Péchot, N., Bardoux, G., Mariotti, A., 2010. Thermal alteration of organic matter during a shrubland fire: a field study. Org. Geochem. 41, 690–697. https://doi.org/10.1016/j.orggeochem.2010.03.003

Almendros, G., González–Vila, F.J., 2012. Wildfires, soil carbon balance and resilient organic matter in Mediterranean ecosystems. A review. Span. J. Soil Sci. 2, 8–33. https://doi.org/10.3232/SJSS.2012.V2.N2.01

Amelung, W., Zech, W., Zhang, X., Follett, R.F., Tiessen, H., Knox, E., Flach, K.W., 1998. Carbon, nitrogen, and sulfur pools in particle–size fractions as influenced by climate. Soil Sci. Soc. Am. J. 62, 172–181. https://doi.org/10.2136/sssaj1998.03615995006200010023x

Armas–Herrera, C.M., Martí, C., Badía, D., Ortiz–Perpiñá, O., Girona–García, A., Mora, J.L., 2018. Short–term and midterm evolution of topsoil organic matter and biological properties after prescribed burning for pasture recovery (Tella, Central Pyrenees, Spain). Land Degrad. Dev. 29, 1545–1554. https://doi.org/10.1002/ldr.2937

Badía–Villas, D., González–Pérez, J.A., Aznar, J.M., Arjona–Gracia, B., Martí–Dalmau, C., 2014. Changes in water repellency, aggregation and organic matter of a mollic horizon burned in laboratory: soil depth affected by fire. Geoderma 213, 400–407. https://doi.org/10.1016/j.geoderma.2013.08.038

Bardgett, R.D., Bowman, W.D., Kaufmann, R., Schmidt, S.K., 2005. A temporal approach to linking aboveground and belowground ecology. Trends Ecol. Evol. 20, 634–641. https://doi.org/10.1016/j.tree.2005.08.005

Bell, T., Adams, M., 2008. Smoke from wildfires and prescribed burning in Australia: effects on human health and ecosystems, in: Bytnerowicz, A., Arbaugh, M.J., Riebau, A.R., Andersen, C. (Eds.), Wildland Fires and Air Pollution. Elsevier, Amsterdam, pp. 289–316. https://doi.org/10.1016/S1474-8177(08)00014-4

Berg, B., McClaugherty, C., 2014. Plant Litter. Decomposition, Humus Formation, Carbon Sequestration, third ed. Springer, Berlin–Heidelberg. https://doi.org/10.1007/978-3-642-38821-7

Bing, H., Wu, Y., Zhou, J., Sun, H., Luo, J., Wang, J., Yu, D., 2016. Stoichiometric variation of carbon, nitrogen, and phosphorus in soils and its implication for nutrient limitation in alpine ecosystem of Eastern Tibetan Plateau. J. Soils Sediments 16, 405–416. https://doi.org/10.1007/s11368-015-1200-9

695 Bodí, M.B., Martin, D.A., Balfour, V.N., Santín, C., Doerr, S.H., Pereira, P., Cerdà, A.,
696 Mataix–Solera, J., 2014. Wildland fire ash: production, composition and eco–hydro–
697 geomorphic effects. Earth–Sci. Rev. 130, 103–127.
698 https://doi.org/10.1016/j.earscirev.2013.12.007
699 Bojko, O., Kabala, C., 2017. Organic carbon pools in mountain soils – Sources of
700 variability and predicted changes in relation to climate and land use changes. Catena 149,
701 209–220. https://doi.org/10.1016/j.catena.2016.09.022
702 Bremner, J.M., 1965. Inorganic forms of nitrogen, in Black, C.A., Evans, D.D., White, J.L.,
703 Ensminger, L.E., Clarck, F.E. (Eds.), Methods of Soil Analysis. Part 2. Agronomy 9.
704 American Society of Agronomy, Madison WI, pp. 1179–1237.
705 Butler, O.M., Lewis, T., Chen, C., 2017. Fire alters soil labile stoichiometry and litter
706 nutrients in Australian eucalypt forests. Int. J. Wildland Fire 26, 783–788.
707 https://doi.org/10.1071/WF17072
708 Caon, L., Vallejo, V.R., Ritsema, C.J., Geissen, V., 2014. Effects of wildfire on soil
709 nutrients in Mediterranean ecosystems. Earth–Sci. Rev. 139, 47–58.
710 https://doi.org/10.1016/j.earscirev.2014.09.001
711 Clement, J.C., Robson, T.M., Guillemin, R., Saccone, P., Lochet, J., Aubert, S., Lavorel,
712 S., 2012. The effects of snow–N deposition and snowmelt dynamics on soil–N cycling in
713 marginal terraced grasslands in the French Alps. Biogeochemistry 108, 297–315.
714 https://doi.org/10.1007/s10533-011-9601-3
715 Costa, D., Pomeroy, J., Baulch, H., Elliott, J., Wheater, H., 2019. Using an inverse
716 modelling approach with equifinality control to investigate the dominant controls on
717 snowmelt nutrient export. Hydrol. Process. 33, 2958–2977.
718 https://doi.org/10.1002/hyp.13463

719 Dijkstra, F.A., Adams, M.A., 2015. Fire eases imbalances of nitrogen and phosphorus in
720 woody plants. Ecosystems 18, 769–779. https://doi.org/10.1007/s10021-015-9861-1
721 Faerber, J., 2009. Prescribed range burning in the Pyrenees: From a traditional practice to
722 a modern management tool. Int. For. Fire News 38, 12–22.
723 Favilli, F., Cherubini, P., Collenberg, M., Egli, M., Sartori, G., Schoch, W., Haeberli, W.,
724 2010. Charcoal fragments of Alpine soils as an indicator of landscape evolution during the
725 Holocene in Val di Sole (Trentino, Italy). Holocene 20, 67–79.
726 https://doi.org/10.1177/0959683609348850
727 Fernandes, P.M., Davies, G.M., Ascoli, D., Fernández, C., Moreira, F., Rigolot, E., Stoof,
728 C.R., Vega, J.A., Molina, D., 2013. Prescribed burning in southern Europe: developing fire
729 management in a dynamic landscape. Front. Ecol. Environ. 11, e4–e14.
730 https://doi.org/10.1890/120298
731 Fernández, I., Cabaneiro, A., Carballas, T., 2001. Thermal resistance to high temperatures
732 of different organic fractions from soils under pine forests. Geoderma 104, 281–298.
733 https://doi.org/10.1016/S0016-7061(01)00086-6
734 Gavazov, K.S., 2010. Dynamics of alpine plant litter decomposition in a changing climate.
735 Plant Soil 337, 19–32. https://doi.org/10.1007/s11104-010-0477-0
736 Garcia–Pausas, J., Romanyà, J., Montané, F., Rios, A.I., Taull, M., Rovira, P., Casals, P.,
737 2017. Are soil carbon stocks in mountain grasslands compromised by land–use changes?,
738 in Catalan, J., Ninot, J.M., Aniz, M. (Eds.), High Mountain Conservation in a Changing
739 World. Springer, Cham, pp. 207–230. https://doi.org/10.1007/978-3-319-55982-7_9
740 Girona–García, A., Badía–Villas, D., Martí–Dalmau, C., Ortiz–Perpiñá, O., Mora, J.L.,
741 Armas–Herrera, C.M., 2018a. Effects of prescribed fire for pasture management on soil
742 organic matter and biological properties: A 1–year study case in the Central Pyrenees. Sci.
743 Total Environ. 618, 1079–1087. https://doi.org/10.1016/j.scitotenv.2017.09.127

744 Girona–García, A., Ortiz–Perpiñá, O., Badía–Villas, D., Martí–Dalmau, C., 2018b. Effects
745 of prescribed burning on soil organic C, aggregate stability and water repellency in a
746 subalpine shrubland: Variations among sieve fractions and depths. Catena 166, 68–77.
747 https://doi.org/10.1016/j.catena.2018.03.018
748 Girona–García, A., Zufiaurre Galarza, R., Mora, J.L., Armas–Herrera, C.M., Martí, C.,
749 Ortiz–Perpiñá, O., Badía–Villas, D., 2018c . Effects of prescribed burning for pasture
750 reclamation on soil chemical properties in subalpine shrublands of the Central Pyrenees
751 (NE–Spain). Sci. Total Environ. 644, 583–593.
752 https://doi.org/10.1016/j.scitotenv.2018.06.363
753 Girona–García, A., Ortiz–Perpiñá, O., Badía–Villas, D., 2019. Dynamics of topsoil carbon
754 stocks after prescribed burning for pasture restoration in shrublands of the Central Pyrenees
755 (NE–Spain). J. Environ. Manag. 233, 695–705.
756 https://doi.org/10.1016/j.jenvman.2018.12.057
757 González–Pérez, J.A., González–Vila, F.J., Almendros, G., Knicker, H., 2004. The effect
758 of fire on soil organic matter – a review. Environ. Int. 30, 855–870.
759 https://doi.org/10.1016/j.envint.2004.02.003
760 González–Sampériz, P., Aranbarri, J., Pérez–Sanz, A., Gil–Romera, G., Moreno, A.,
761 Leunda, M., Sevilla–Callejo, M., Corella, J.P., Morellón, M., Oliva, B., Valero–Garcés, B.,
762 2017. Environmental and climate change in the southern Central Pyrenees since the Last
763 Glacial Maximum: A view from the lake records. Catena 149, 668–688.
764 https://doi.org/10.1016/j.catena.2016.07.041
765 Gray, D.M., Dighton, J., 2006. Mineralization of forest litter nutrients by heat and
766 combustion. Soil Biol. Biochem. 38, 1469–1477.
767 https://doi.org/10.1016/j.soilbio.2005.11.003

768 Güsewell, S., 2004. N: P ratios in terrestrial plants: variation and functional significance.
769 New Phytol. 164, 243–266. https://doi.org/10.1111/j.1469-8137.2004.01192.x
770 Hagedorn, F., Schleppi, P., Bucher, J., Flühler, H., 2001. Retention and leaching of elevated
771 N deposition in a forest ecosystem with Gleysols. Water Air Soil Pollut. 129, 119–142.
772 https://doi.org/10.1023/A:1010397232239
773 Hagedorn, F., Mulder, J., Jandl, R., 2010. Mountain soils under a changing climate and
774 land–use. Biogeochemistry 97, 1–5. https://doi.org/10.1007/s10533-009-9386-9
775 Hobley, E., 2019. Vertical distribution of soil pyrogenic matter: a review. Pedosphere 29,
776 137–149. https://doi.org/10.1016/S1002-0160(19)60795-2
777 Huang, W., Xu, Z., Chen, C., Zhou, G., Liu, J., Abdullah, K.M., Reverchon, F., Liu, X.,
778 2013. Short–term effects of prescribed burning on phosphorus availability in a suburban
779 native forest of subtropical Australia. J. Soils Sediments 13, 869–876.
780 https://doi.org/10.1007/s11368-013-0660-z
781 Jensen, L.S., Salo, T., Palmason, F., Breland, T.A., Henriksen, T.M., Stenberg, B.,
782 Pedersen, A., Lundstrom, C., Esala, M., 2005. Influence of biochemical quality on C and
783 N mineralisation from a broad variety of plant materials in soil. Plant Soil 273, 307–326.
784 https://doi.org/10.1007/s11104-004-8128-y
785 Jiménez–Morillo, N.T., de la Rosa, J.M., Waggoner, D., Almendros, G., González–Vila,
786 F.J., González–Pérez, J.A., 2016. Fire effects in the molecular structure of soil organic
787 matter fractions under *Quercus suber* cover. Catena 145, 266–273.
788 https://doi.org/10.1016/j.catena.2016.06.022
789 Kalra, I.P., Maynard, D.G., 1991. Methods for Forest Soil and Plant Analysis. Forestry
790 Canada, Northwest Region, Northern Forestry Centre, Edmonton.

Koerselman, W., Meuleman, A.F.M., 2006. The vegetation N:P ratio: a new tool to detect the nature of nutrient limitation. J. Appl. Ecol. 33, 1441–1450. https://doi.org/10.2307/2404783

Kozłowska–Strawska, J., Kaczor, A., 2009. Sulphur as a deficient element in agriculture–its influence on yield and on the quality of plant materials. Ecol. Chem. Engineer. A 16, 9–19.

Kull, C.A., 2008. Landscapes of fire: origins, politics, and questions, in: David, B., Thomas, J. (Eds.), Handbook of Landscape Archaeology. Routledge, London–New York, pp. 424–429.

Kwiatkowska–Malina, J., 2018. Qualitative and quantitative soil organic matter estimation for sustainable soil management. J. Soils Sediments 18, 2801–2812. https://doi.org/10.1007/s11368-017-1891-1

Makarov, M.I., Leoshkina, N.A., Ermak, A.A., Malysheva, T.I., 2010. Seasonal dynamics of the mineral nitrogen forms in mountain–meadow alpine soils. Eurasian Soil Sci. 43, 905–913. https://doi.org/10.1134/S1064229310080077

Marinas, A., García–González, R., Fondevila M., 2003. The nutritive value of five pasture species occurring in the summer grazing ranges of the Pyrenees. Anim. Sci. 76, 461–469. https://doi.org/10.1017/S1357729800058689

Martínez–Vilalta, J., Sala, A., Asensio, D., Galiano, L., Hoch, G., Palacio, S., Piper, F.I., Lloret, F., 2016. Dynamics of non–structural carbohydrates in terrestrial plants: a global synthesis. Ecol. Monogr. 86, 495–516. https://doi.org/10.1002/ecm.1231

Merino, A., Chávez–Vergara, B., Salgado, J., Fonturbel, M.T., García–Oliva, F., Vega, J.A., 2015. Variability in the composition of charred litter generated by wildfire in different ecosystems. Catena 133, 52–63. https://doi.org/10.1016/j.catena.2015.04.016

Mora, J.L., Armas, C., Badía, D., Montserrat, G., Palacio, S., Gómez D., 2018. Assessment of the bromatological quality of thorny cushion dwarf after prescribed fire for pasture improvement in Central Pyrenees (in Spanish, with English abstract), in: Roig, S., Barrrantes, O. (Eds.), Pastoralismo y Vías Pecuarias. Conectando Tradición e Innovación. Sociedad Española de Pastos, Teruel, pp. 142–150.

Múgica, L., Canals, R.M., San Emeterio, L., 2018. Changes in soil nitrogen dynamics caused by prescribed fires in dense gorse lands in SW Pyrenees. Sci. Total Environ. 639, 175–185. https://doi.org/10.1016/j.scitotenv.2018.05.139

Murphy, J., Riley, J.P. 1962. A modified single solution method for the determination of phosphate in natural waters. Anal. Chim. Acta 27, 31–36. https://doi.org/10.1016/S0003-2670(00)88444-5

Naisse, C., Girardin, C., Lefevre, R., Pozzi, A., Maas, R., Stark, A., Rumpel, C., 2015. Effect of physical weathering on the carbon sequestration potential of biochars and hydrochars in soil. Glob. Change Biol. Bioenergy 7, 488–496. https://doi.org/10.1111/gcbb.12158

Nuche, P., Gartzia, M., Vilellas, J., Reiné, R., Alados, C.L., 2018. Assessment of prescribed fire and cutting as means of controlling the invasion of subalpine grasslands by *Echinospartum horridum*. Appl. Veg. Sci. 21, 198–206. https://doi.org/10.1111/avsc.12354

Neary, D.G., Klopatek, C.C., DeBano, L.F., Ffolliott, P.F., 1999. Fire effects on belowground sustainability: a review and synthesis. For. Ecol. Manag. 122, 51–71. https://doi.org/10.1016/S0378-1127(99)00032-8

Onyiah, L.C., 2008. Design and Analysis of Experiments: Classical and Regression Approaches with SAS. CRC Press, Boca Raton FL. https://doi.org/10.1201/b15920

Pereira, P., Brevik, E., Bogunovic, I., Estebaranz–Sánchez, F. 2019. Ash and soils: a close relationship in fire–affected areas, in: Pereira, P., Mataix–Solera, J., Úbeda, X., Rein, G.,

Cerdà, A., Rein, G. (Eds.) Fire Effects on Soil Properties. CSIRO, Clayton South–Leiden, pp. 39–68. https://doi.org/10.1071/9781486308149

Prescott, C.E., 2005. Decomposition and mineralization of nutrients from litter and humus, in: BassiriRad, H. (Ed.), Nutrient Acquisition by Plants. An Ecological Perspective. Springer, Berlin–Heidelberg, pp. 15–41. https://doi.org/10.1007/3-540-27675-0_2

Preston, C.M., Schmidt, M.W., 2006. Black (pyrogenic) carbon: a synthesis of current knowledge and uncertainties with special consideration of boreal regions. Biogeosciences 3, 397–420. https://doi.org/10.5194/bg-3-397-2006

Prietzel, J., Christophel, D., 2014. Organic carbon stocks in forest soils of the German Alps. Geoderma 221, 28–39. https://doi.org/10.1016/j.geoderma.2014.01.021

Puissant, J., Mills, R.T.E., Robroek, B.J.M., Gavazov, K., Perrette, Y., De Danieli, S., Spiegelberger, T., Buttler, A., Brun, J.J., Cécillon, L., 2017. Climate change effects on the stability and chemistry of soil organic carbon pools in a subalpine grassland. Biogeochemistry 132, 123–139. https://doi.org/10.1007/s10533-016-0291-8

Pyke, D.A., 2003. Coordinated intermountain restoration project−fire, decomposition and restoration, in: Allsopp, N., Palmer, A.R., Milton, S.J., Kirkman, K.P., Kerley, G.I.H., Hurt, C.R., Brown C.J. (Eds.), Proceedings of the VIIth International Rangelands Congress, Durban, pp. 1116–1124.

Raison, R.J., Khanna, P.K., Woods, P.V., 1985. Mechanisms of element transfer to the atmosphere during vegetation fires. Can. J. For. Res. 15, 132–140. https://doi.org/10.1139/x85-022

Rhoades, J.D., 1982. Soluble salts, in Page, A.L., Miller, R.H., & Keeney, D.R. (Eds.), Methods of Soil Analysis. Part 2. American Society of Agronomy–Soil Science Society of America, Madison WI, pp. 167–179.

Ripoll, A., Minguillón, M.C., Pey, J., Jimenez, J.L., Day, D.A., Sosedova, Y., Canonaco, F., Prévôt, A.S.H., Querl, X., Alastuey, A., 2015. Long–term real–time chemical characterization of submicron aerosols at Montsec (southern Pyrenees, 1570 m asl). Atmos. Chem. Phys. 15, 2935–2951. https://doi.org/10.5194/acp-15-2935-2015

Saenger, A., Cécillon, L., Poulenard, J., Bureau, F., De Daniéli, S., Gonzalez, J.M., Brun, J.J., 2015. Surveying the carbon pools of mountain soils: A comparison of physical fractionation and Rock–Eval pyrolysis. Geoderma 241, 279–288. https://doi.org/10.1016/j.geoderma.2014.12.001

Santín, C., Doerr, S.H., 2016. Fire effects on soils: the human dimension. Philos. Trans. R. Soc. Lond. B Biol. Sci. 371, 20150171. https://doi.org/10.1098/rstb.2015.0171

Thonicke, K., Venevsky, S., Sitch, S., Cramer, W., 2001. The role of fire disturbance for global vegetation dynamics: coupling fire into a dynamic global vegetation model. Glob. Ecol. Biogeogr. 10, 661–677. https://doi.org/10.1046/j.1466-822X.2001.00175.x

Tiedemann, A.R., 1987. Combustion losses of sulfur from forest foliage and litter. For. Sci. 33, 216–223. https://doi.org/10.1093/forestscience/33.1.216

Toberman, H., Chen, C., Lewis, T., Elser, J.J., 2014. High–frequency fire alters C: N: P stoichiometry in forest litter. Glob. Change Biol. 20, 2321–2331. https://doi.org/10.1111/gcb.12432

Ward, A., Dargusch, P., Thomas, S., Liu, Y., Fulton, E.A., 2014. A global estimate of carbon stored in the world's mountain grasslands and shrublands, and the implications for climate policy. Glob. Environ. Change 28, 14–24. https://doi.org/10.1016/j.gloenvcha.2014.05.008

Watanabe, F.S., Olsen, S.R., 1965. Test of an ascorbic acid method for determining phosphorus in water and $NaHCO_3$ extracts from soil. Soil Sci. Soc. Am. J 29, 677–678. https://doi.org/10.2136/sssaj1965.03615995002900060025x

889 Weintraub, M.N., 2011. Biological phosphorus cycling in arctic and alpine soils, in:
890 Bünemann, E., Oberson, A., Frossard, E. (Eds.), Phosphorus in Action. Biological
891 Processes in Soil Phosphorus Cycling. Springer, Berlin–Heidelberg, pp. 295–316.
892 https://doi.org/10.1007/978-3-642-15271-9_12
893 Yang, H., Yan, R., Chen, H., Lee, D.H., Zheng, C., 2007. Characteristics of hemicellulose,
894 cellulose and lignin pyrolysis. Fuel 86, 1781–1788.
895 https://doi.org/10.1016/j.fuel.2006.12.013

FIGURE CAPTIONS

Figure 1 Images of the study site before (a) and during (b) burning; of the soil surface after burning (c, d); and of the study site 6 (e), 12 (f), 18 (g), and 24 months (h) after burning.

Figure 2 Schematic diagram of the main analyses carried out on the litter, duff, ash, and soil samples collected immediately before (preburn) and after burning (T0) and 6, 12, 18, and 24 months after burning (T6, T12, T18, and T24). OM = organic matter, POM = particulate organic matter.

Figure 3 Postburn evolution of the proportions (mean ± standard error) of nonstructural, hemicellulose, cellulose, lignin-type, and nonparticulate organic matter (NPOM) of the litter and duff layers and of the topsoil in the 0–1, 1–2, 2–3, and 3–5 cm depths. The headings of the columns denote the sampling time: immediately before (preburn) and after burning (T0) and 6, 12, 18, and 24 months after fire (T6, T12, T18, and T24). Within each layer or depth, values followed by the same letter do not differ among sampling periods.

Figure 4 Mean changes (± standard deviation) resulting from combustion and apparent enrichment in the concentrations of the particulate (POM) and nonparticulate (NPOM) organic matter (a), particulate (POC) and nonparticulate (NPOC) organic carbon (b), and particulate (PON) and nonparticulate (NPON) nitrogen (c) in the topsoil at the 0–1, 1–2, 2–3, and 3–5 cm depths. The headings of the columns denote the sampling time: immediately before (preburn) and after burning (T0) and 6, 12, 18, and 24 months after burning (T6, T12, T18, and T24). Values (mean ± SD) are expressed relative to the initial (preburn) concentrations.

Figure 5 Postburn evolution of the concentrations (mean ± standard error) of the particulate (POC) and nonparticulate (NPOC) organic carbon (a), particulate (PON) and nonparticulate (NPON) nitrogen (b), particulate organic phosphorus (POP) (c), and particulate organic sulfur (POS) (d) in the topsoil at the 0–1, 1–2, 2–3, and 3–5 cm depths. The headings of the

columns denote the sampling time: immediately before (preburn) and after burning (T0) and 6, 12, 18, and 24 months after burning (T6, T12, T18, and T24). Within each depth, the values followed by the same letter do not differ among sampling periods.

Figure 6 Postburn evolution of the values (mean ± standard error) of the C:N ratio of the litter and duff layers and of the particulate (POM) and nonparticulate (NPOM) organic matter of the topsoil in the 0–1, 1–2, 2–3 and 3–5 cm depths; and of the C:P (b), C:S (c), N:P (d), N:S (e), and P:S (f) ratios of the litter and duff layers and of the POM in the topsoil in the 0–1, 1–2, 2–3 and 3–5 cm depths. The headings of the columns denote the sampling time: immediately before (preburn) and after burning (T0) and 6, 12, 18, and 24 months after burning (T6, T12, T18, and T24). Within each layer or depth, the values followed by the same letter do not differ among sampling periods.

Figure 7 Postburn evolution of the soil properties (mean ± standard error) in the topsoil at the 0–1, 1–2, 2–3, and 3–5 cm depths for (a) electric conductivity, (b) pH and concentrations of ammonium–N (c), nitrate–N (d), Olsen–P (e), and water–soluble S (f). The headings of the columns denote the sampling time: immediately before (preburn) and after burning (T0) and 6, 12, 18, and 24 months after burning (T6, T12, T18, and T24). Within each depth, the values followed by the same letter do not differ significantly between sampling periods.

939 **Table 1** Chemical composition (mean ± standard deviation) of the ash in comparison with
940 that of the litter layer before the fire along with the average values of the fine twigs of
941 *Echinospartum horridum* reported by Marinas et al. (2003) (1) and Mora et al. (2018) (2).

	Ash	OL layer	Twigs of *E. horridum*	
			(1)	(2)
pH (1: 2.5 solid: water)	11.6 ± 0.8			
Electric cond. ($mS \cdot cm^{-1}$, 1: 5)	8.8 ± 2.0			
Carbonates ($g \cdot kg^{-1}$)	325 ± 45			
Ammonium–N ($mg \cdot kg^{-1}$)	38.4 ± 1.7			
Nitric–N ($mg \cdot kg^{-1}$)	6.6 ± 0.6			
Olsen–P ($mg \cdot kg^{-1}$)	419 ± 32			
Soluble S ($mg \cdot kg^{-1}$)	1254 ± 710			
Total P ($g \cdot kg^{-1}$)	9.89 ± 7.05	0.27 ± 0.03		0.38 ± 0.10
Total S ($g \cdot kg^{-1}$)	5.79 ± 1.85	0.86 ± 0.07		0.28 ± 0.08
Total organic matter ($g \cdot kg^{-1}$)	223 ± 90	948 ± 7		967 ± 6
Total organic–C ($g \cdot kg^{-1}$)	131 ± 46	431 ± 28		
Total N ($g \cdot kg^{-1}$)	6.87 ± 3.14	14.2 ± 1.08	15.7 ± 6.1	17.0 ± 1.5
C:N ratio	20.5 ± 3.1	31.2 ± 1.4		
C:P ratio	20 ± 13	1600 ± 100		
C:S ratio	25 ± 13	501 ± 35		
N:P ratio	1.1 ± 0.8	52.7 ± 5.6		46.4 ± 10.3
N:S ratio	1.4 ± 0.8	16.5 ± 1.9		6.5 ± 1.7
P:S ratio	1.58 ± 0.61	0.31 ± 0.01		1.43 ± 0.45
Lignin (% of organic matter)	69.2 ± 9.3	29.3 ± 1.1	18.6 ± 3.4	15.2 ± 0.5
Cellulose (% of organic matter)	21.3 ± 6.3	24.0 ± 5.7	26.3 ± 5.0	32.6 ± 0.6

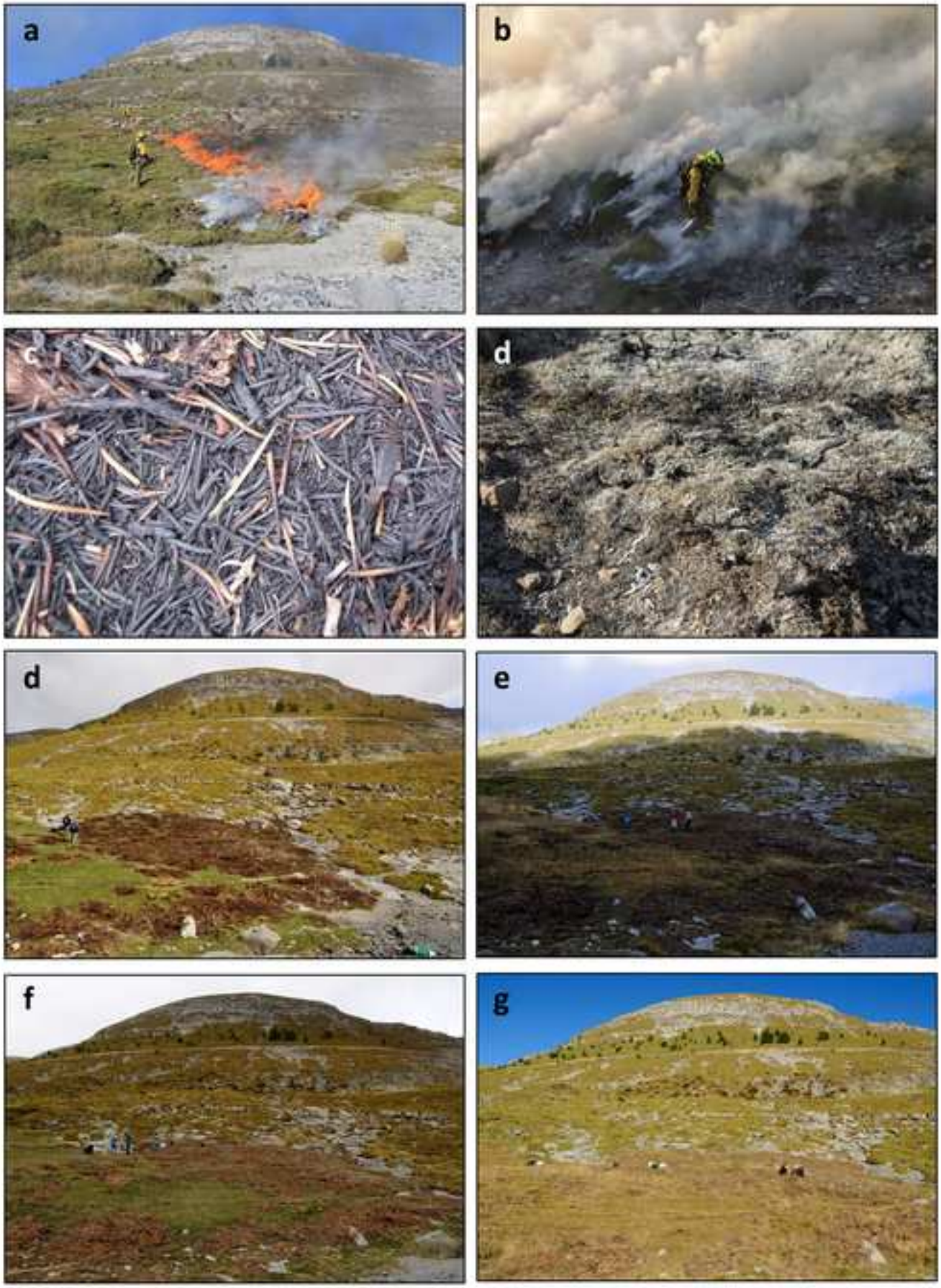

Fig. 1

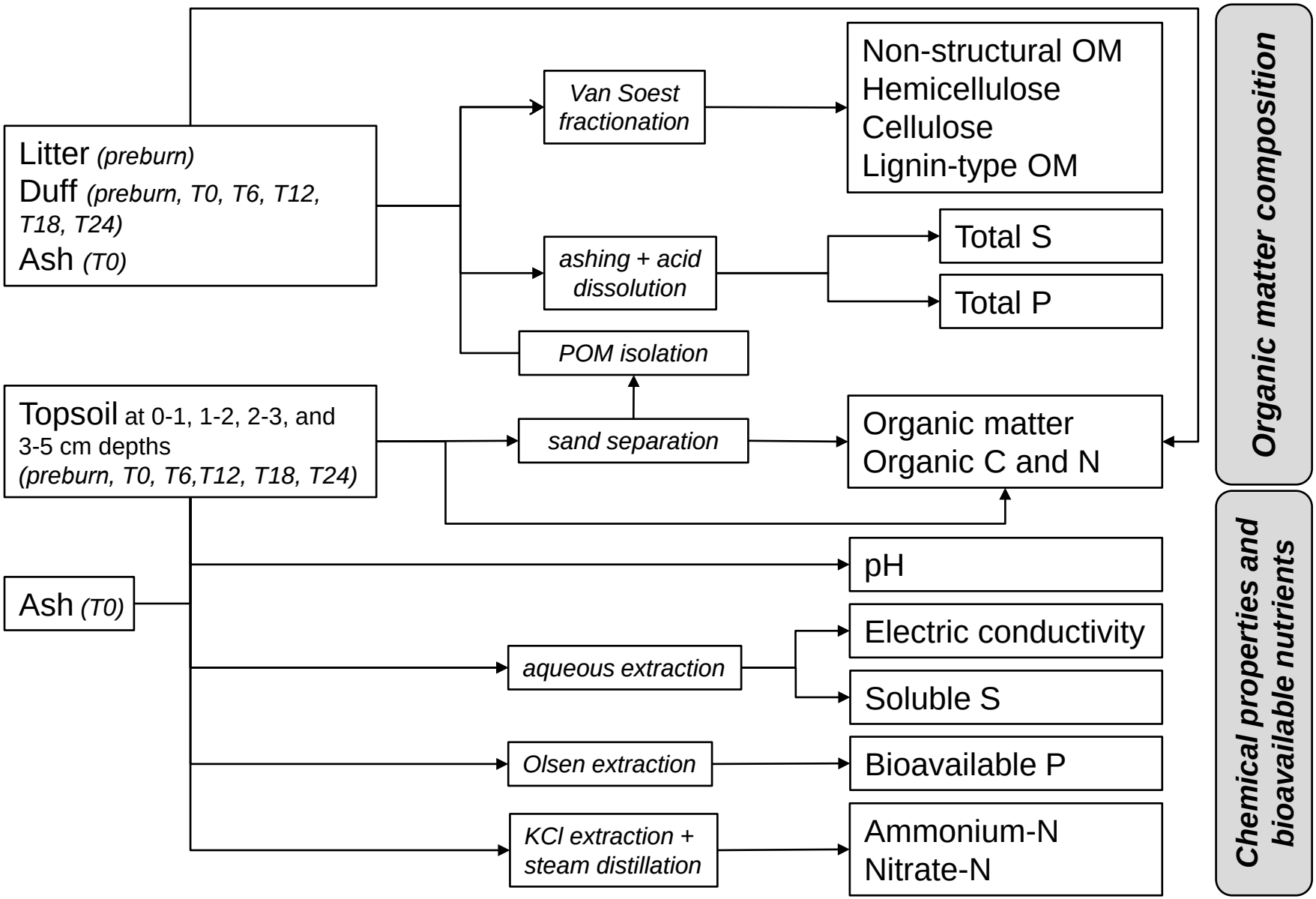
Litter (preburn)
Duff (preburn, T0, T6, T12, T18, T24)
Ash (T0)
Van Soest fractionation
Non-structural OM
Hemicellulose
Cellulose
Lignin-type OM
ashing + acid dissolution
Total S
Total P
POM isolation
Topsoil at 0-1, 1-2, 2-3, and 3-5 cm depths (preburn, T0, T6,T12, T18, T24)
sand separation
Organic matter
Organic C and N
Organic matter composition
Ash (T0)
pH
Electric conductivity
aqueous extraction
Soluble S
Olsen extraction
Bioavailable P
KCl extraction + steam distillation
Ammonium-N
Nitrate-N
Chemical properties and bioavailable nutrients

Fig. 2

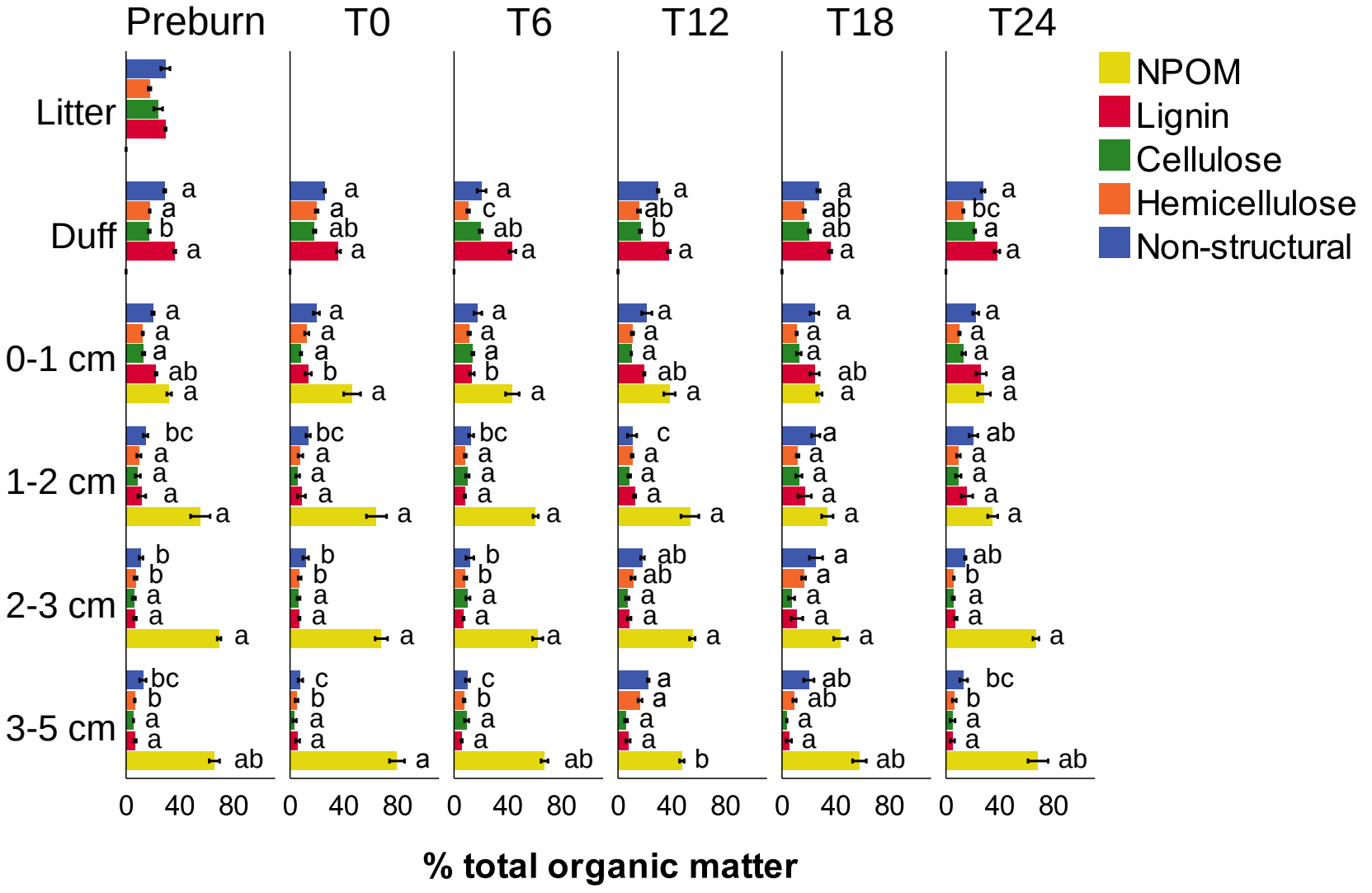
Preburn
T0
T6
T12
T18
T24
Litter
Duff
0-1 cm
1-2 cm
2-3 cm
3-5 cm
NPOM
Lignin
Cellulose
Hemicellulose
Non-structural
0
40
80
% total organic matter

Fig. 3

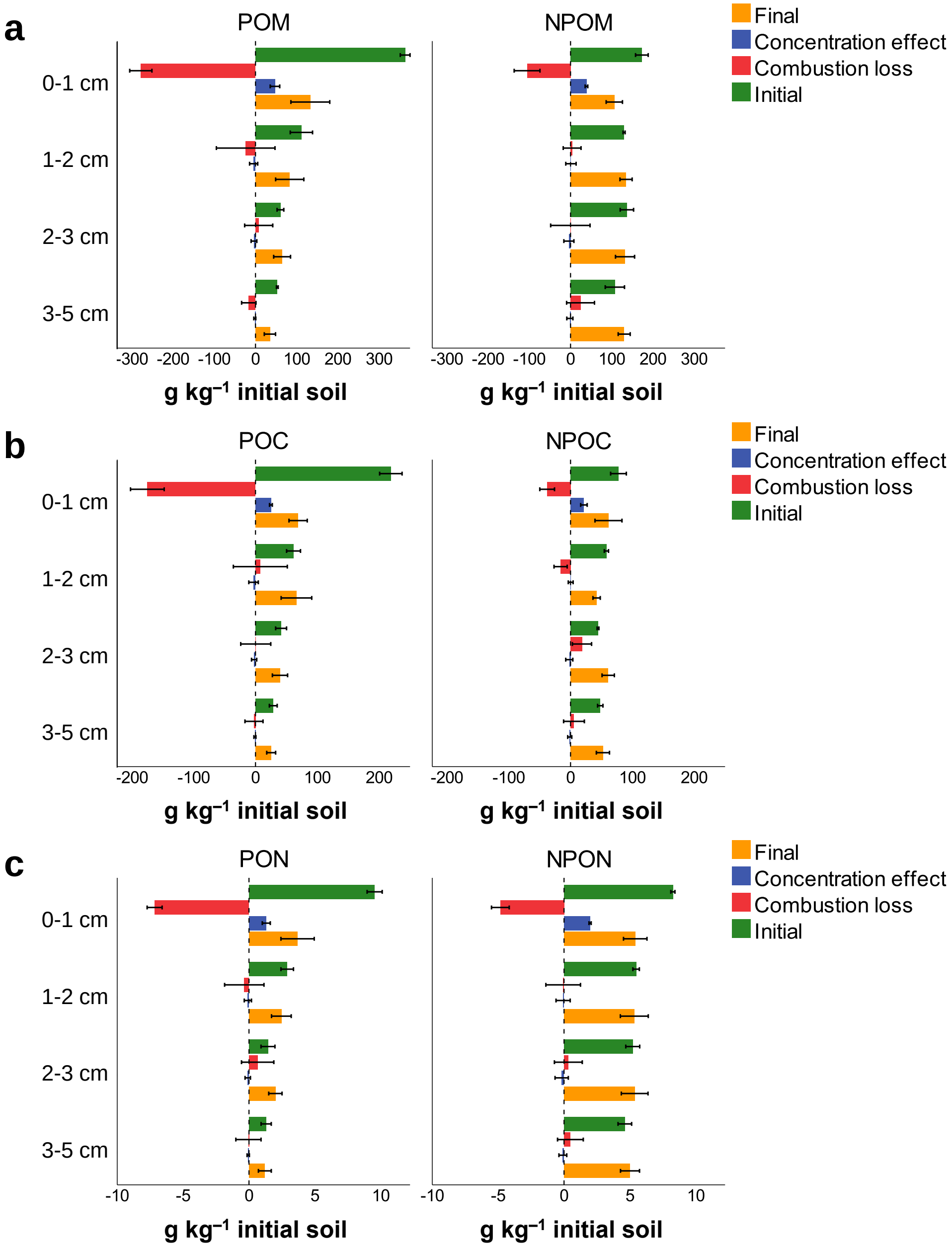
a
POM
NPOM
Final
Concentration effect
Combustion loss
Initial
0-1 cm
1-2 cm
2-3 cm
3-5 cm
-300 -200 -100 0 100 200 300
g kg⁻¹ initial soil
b
POC
NPOC
-200 -100 0 100 200
c
PON
NPON
-10 -5 0 5 10

Fig. 4

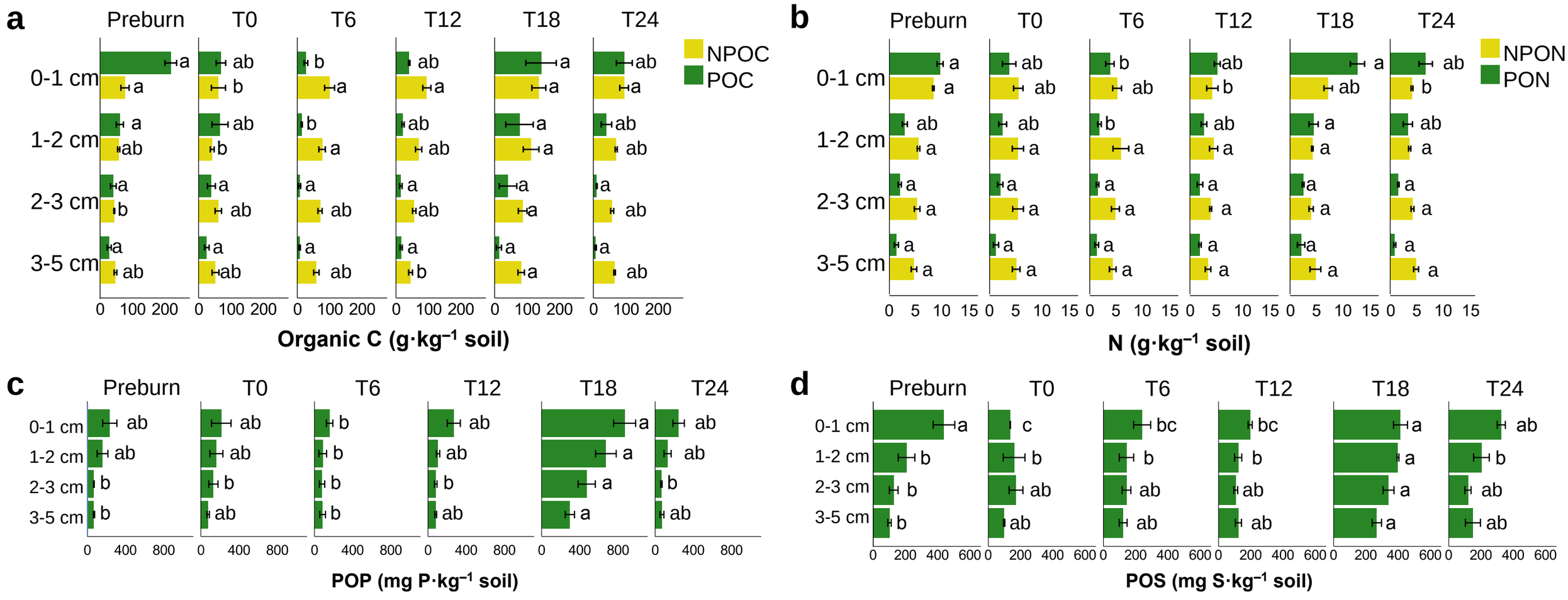
a
Preburn
T0
T6
T12
T18
T24
0-1 cm
1-2 cm
2-3 cm
3-5 cm
NPOC
POC
0 100 200
Organic C (g·kg⁻¹ soil)
b
NPON
PON
0 5 10 15
N (g·kg⁻¹ soil)
c
0 400 800
POP (mg P·kg⁻¹ soil)
d
0 200 400 600
POS (mg S·kg⁻¹ soil)

Fig. 5

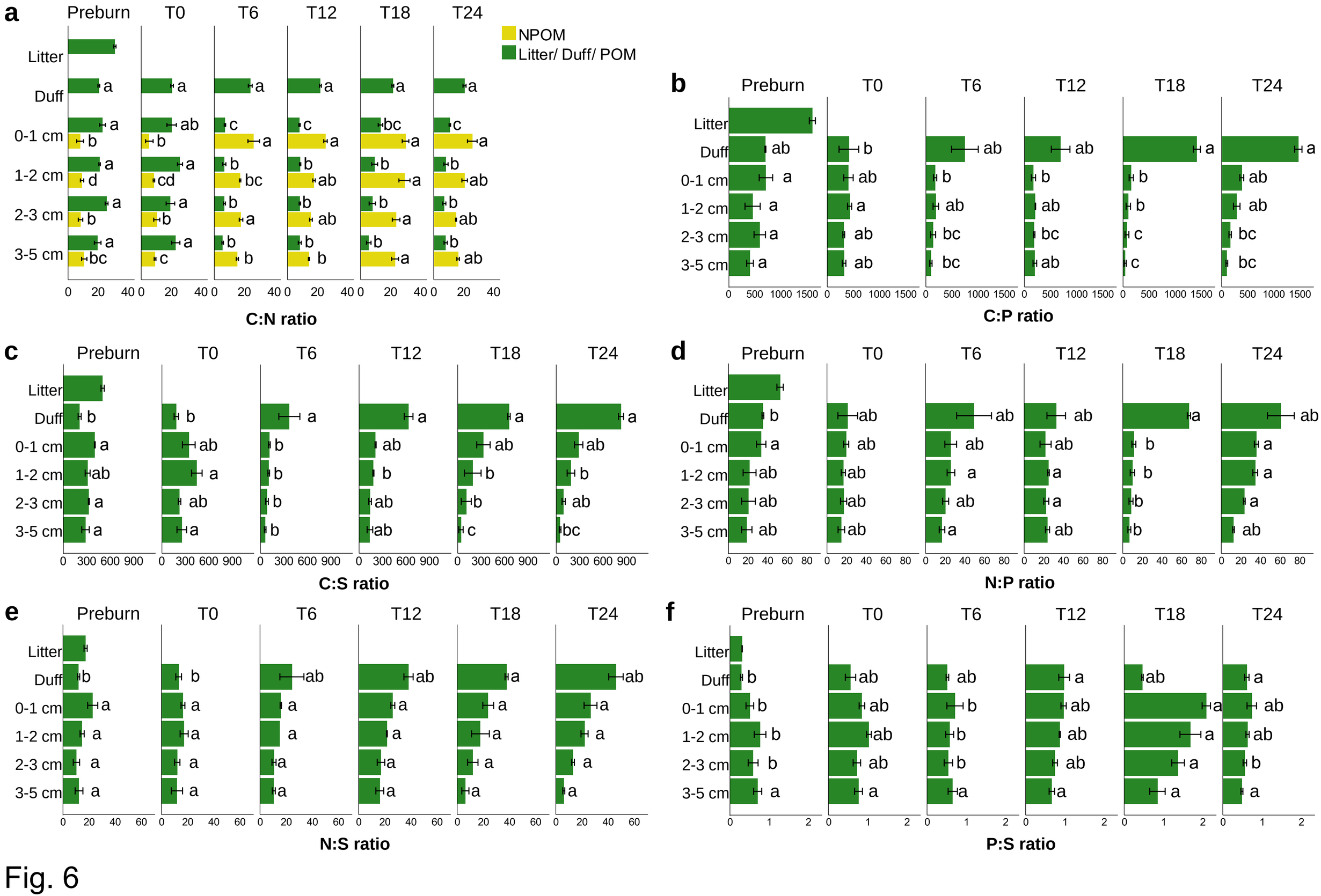
a
Preburn
T0
T6
T12
T18
T24
NPOM
Litter/ Duff/ POM
Litter
Duff
0-1 cm
1-2 cm
2-3 cm
3-5 cm
C:N ratio
b
C:P ratio
c
C:S ratio
d
N:P ratio
e
N:S ratio
f
P:S ratio

Fig. 6

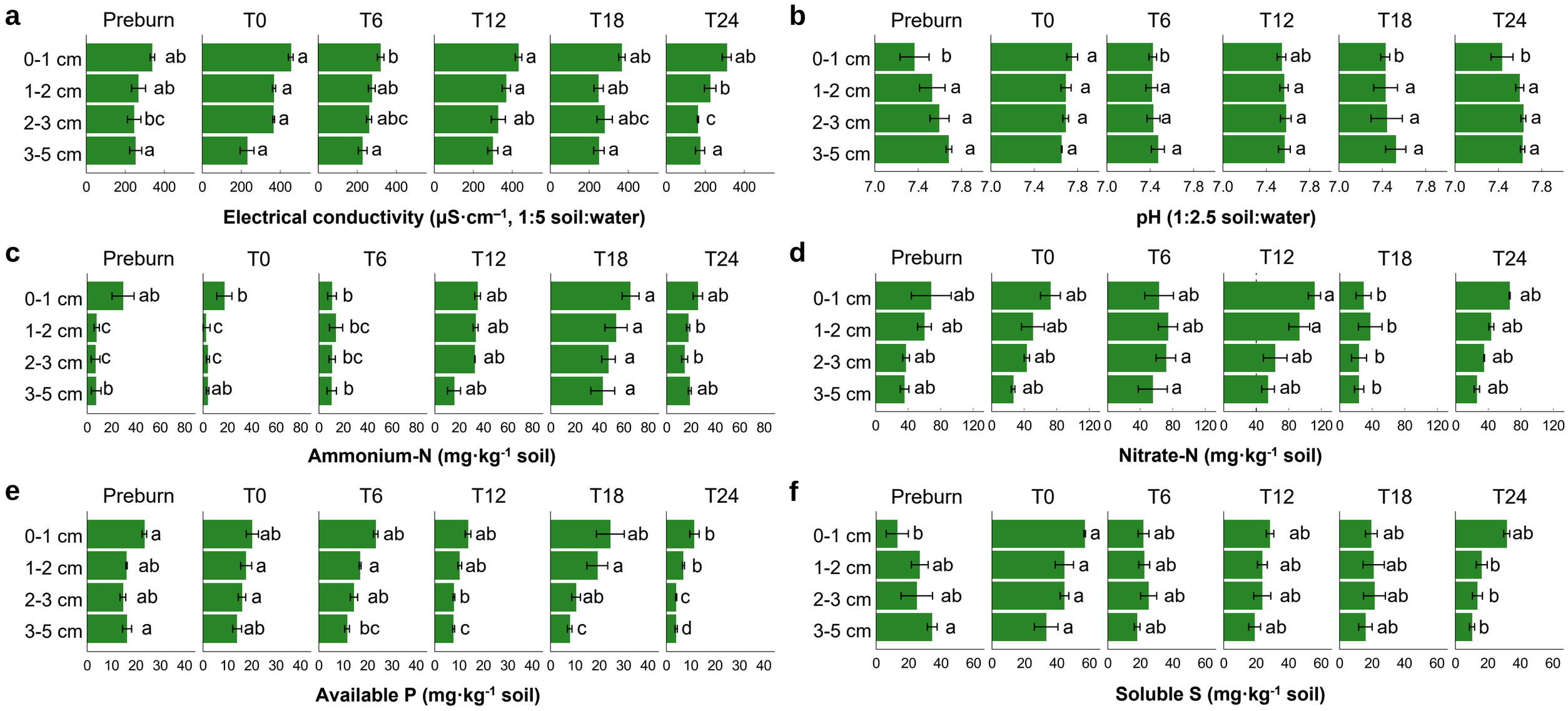
a
Preburn
T0
T6
T12
T18
T24
0-1 cm
1-2 cm
2-3 cm
3-5 cm
Electrical conductivity (μS·cm⁻¹, 1:5 soil:water)
b
pH (1:2.5 soil:water)
c
Ammonium-N (mg·kg⁻¹ soil)
d
Nitrate-N (mg·kg⁻¹ soil)
e
Available P (mg·kg⁻¹ soil)
f
Soluble S (mg·kg⁻¹ soil)

Fig. 7

HIGHLIGHTS

- Prescribed fire caused considerable C losses at the 0–1 cm depth, mostly from POM
- Uneven combustion resulted in few qualitative changes in the remaining organic matter
- Bioavailable N showed transient increases, while S and P gradually declined after fire
- Steadier nutrient inputs were derived from the breakdown of particulate charcoal